Quantum Coherence in Low-Dimensional Interacting Fermi Systems

Ulrich Eckern and Cosima Schuster

Institute of Physics, University of Augsburg, 86135 Augsburg, Germany

1 Introduction

Disorder versus interaction induced metal-insulator transitions are still a central problem in solid state physics. For non-interacting electrons in disordered systems [1] the scaling hypothesis of localization [2] successfully predicts many of the universal features of the transition from metallic to insulating behavior. However, the influence of the interaction on the transition is not equally well understood [3]; recent investigations of an apparent metal-insulator transition in two-dimensional systems even question the main assumptions of the scaling hypothesis [4]. Hereby, attention is also directed to randomly and periodically distorted one-dimensional systems. In one dimension, an infinitesimal amount of disorder (with backscattering contributions) leads to a localized ground state for non-interacting electrons, but with interaction [5] or for special realizations of the disorder [6,7] this result may change.

In contrast to higher dimensional systems, one-dimensional models are often accessible to a detailed theoretical (analytical and numerical) treatment. Using the density matrix renormalization group (DMRG) algorithm, we investigate a lattice model for spinless fermions as well as the Hubbard model in the presence of various potentials. We determine the ground state energy and the phase sensitivity [8] of a ring of interacting spinless fermions as well as the local density, from which the decay of the Friedel oscillations is obtained. For the Hubbard model, we concentrate on the Friedel oscillations.

We start with a brief review of the effects of a single impurity in an interacting one-dimensional Fermi system. Generalizing these results we discuss how the interplay of disorder and interaction can lead to an extended ground state. For example, spinless fermions and electrons in a special quasi-periodic potential [9] show a metal-insulator transition at a finite potential strength, independent of interaction [10,11], whereas the phase diagrams in the presence of random [12] and periodic potentials [13] show a delocalized phase for strong attractive interactions only. The investigation of interacting-electron models is more difficult: The phase sensitivity, a very practical observable in the spinless-fermion case, cannot be used for the Hubbard model [14]. For this case, we hence characterize our system through the Friedel oscillations; in addition, these should be experimentally accessible.

2 Methods and Models

2.1 Methods

The DMRG is a quasi-exact numerical method to determine the ground state properties, i.e. the ground state and the ground state energy, of long one-dimensional (non-integrable) systems with reasonable accuracy [15]. It is useful to implement the spinless-fermion model in terms of the equivalent spin chain, and the Hubbard model as two coupled spin chains. In particular, we calculate the phase sensitivity, i.e. the reaction of the system to a change in the boundary condition. This quantity is very useful to determine numerically the localization-delocalization transition for systems with finite size. We model the boundary condition via a magnetic flux, which results in an additional phase in the hopping terms. The energy levels depend on the total flux, Φ, only. Thus we determine in particular the energy difference between periodic ($c_N = c_0$, $\Phi = 0$) and anti-periodic ($c_N = -c_0$, $\Phi = \pi$) boundary conditions, $\Delta E = (-)^{N_f}[E(0) - E(\pi)]$. We denote by L the length of the chain, by N the number of sites, and by N_f the number of fermions. The factor $(-1)^{N_f}$ cancels the odd-even effects resulting from the change in the ground state for odd compared to even particle numbers. The phase sensitivity, $N\Delta E$, is independent of N for the metallic state. In an insulator, on the other hand, the system does not feel a twist in the boundary condition, i.e. $N\Delta E$ is expected to decrease with system size. Using the DMRG, it is possible to extend the tractable system lengths for the spin chain to about $N \approx 100 - 200$. In our simulations we perform five lattice sweeps and keep 300 to 500 states per block. Local quantities as e. g. the density can be obtained within an error of 10^{-6} in the Hubbard model when using open boundary conditions, with about 300 states taken into account for chains with about 80 sites. This requires a memory of about 700 MB.

Note that in one dimension, a useful – for the interpretation of the numerical data – formulation on the basis of the bosonization technique [16] is available: The low lying excitations of the non-interacting as well as the interacting fermions are sound waves, i.e. the Fermi system can be described as a non-interacting Bose system, called a Luttinger liquid [17]. The main advantage of the bosonization is that the kinetic and interaction terms are described at the same level, i.e. the Hamiltonian of the interacting Fermi system is diagonalized. Starting from the linearized energy dispersion of non-interacting fermions,

$$H^0 = \sum_{k>0} v_F(k - k_F)c_k^+ c_k + \sum_{k<0} v_F(-k - k_F)c_k^+ c_k \ , \tag{1}$$

it was shown [18] that the bosonic Hamiltonian

$$H_B^0 = \frac{2\pi v_F}{L} \sum_{q>0} [\rho_R(q)\rho_R(-q) + \rho_L(-q)\rho_L(q)] \tag{2}$$

is equivalent to (1). The corresponding (bosonic) phase variables can be introduced in an intuitive way, writing the particle density of the Fermi system as

$$\rho(x) = \sum_i \delta(x - x_i) \to \partial_x \phi \sum_n \delta(\phi(x) - n\pi) \,, \tag{3}$$

and assuming that ϕ increases monotonically by π each time x passes the location of a particle, $x = x_i$, i.e. the particles are thought to be located at the points where $\phi(x) = n\pi$. Creating a particle means introducing a kink of height π into $\phi(x)$. The field operator, ψ^+, is thus a displacement operator, $\exp[i\pi \int_0^x \mathrm{d}x' \Pi(x')]$, see e. g. [19]. Then, by defining $\Pi(x) = \partial_x \theta(x)/\pi$, we obtain

$$\psi^+ = [n_0 + \partial_x \varphi(x)/\pi]^{1/2} \mathrm{e}^{i\theta(x)} \mathrm{e}^{i[k_F x + \varphi(x)]} \,. \tag{4}$$

Here we set $\partial_x \phi(x) = n_0 + \partial_x \varphi(x)/\pi$. The exponential φ-term has to be introduced to achieve the anti-commutation relations of the fermionic operators. With the above definitions, $\varphi(x)$ and $\partial_x \theta(x)/\pi$ are conjugate variables.

2.2 Models

As a first example, we consider a generalized anisotropic Heisenberg (XXZ) model:

$$\begin{aligned} H_{\mathrm{spin}} = &- \sum_{n=1}^{N} J_n(u) \left(\sigma_n^x \sigma_{n+1}^x + \sigma_n^y \sigma_{n+1}^y + \Delta \sigma_n^z \sigma_{n+1}^z \right) \\ &- \sum_n^N h_n \sigma_n^z + N \frac{K}{2} u^2 \,, \end{aligned} \tag{5}$$

where we include an alternating coupling, $J_n(u) = J[1 + (-1)^n u]$; h_n denotes a random magnetic field. The loss in lattice energy due to the dimerization is taken into account within the harmonic approximation with K as stiffness constant. For the clean XXZ model, i.e. for $u = 0$, and for zero total magnetization, $M = \sum_n \langle \sigma_n^z \rangle = 0$, one finds three phases [20]: a ferromagnetic phase for $\Delta \geq 1$, separated by a first-order transition from a gapless phase for $-1 \leq \Delta < 1$ (whose low lying excitations are given by those of a Luttinger liquid); and an antiferromagnetic phase for $\Delta < -1$. The transition from the Luttinger to the antiferromagnetic phase is of Berezinskii-Kosterlitz-Thouless type. The corresponding fermionic model is obtained via the Jordan-Wigner transformation. Changing the notation, $J \to t$, $J\Delta \to -V/2$, and $h_i \to -\epsilon_i/2$, and neglecting constant energy shifts like $\sum_i h_i$ and $\Delta(2N_f - N/2)$, we obtain

$$H_{\mathrm{fermion}} = - \sum_i t_i \left(c_i^+ c_{i+1} + \mathrm{h.\,c.} \right) + \sum_i V_i n_i n_{i+1} + \sum \epsilon_i n_i \,, \tag{6}$$

where $t_i(u) = t[1 + (-1)^i u_t]$, and $V_i(u) = V[1 + (-1)^i u_V]$. The random on-site energies ϵ_i can be considered as due to local impurity potentials. In the bosonized form, the Hamiltonian can be written as follows:

$$H_{\mathrm{B}} = \int \frac{\mathrm{d}x}{2\pi} \Big\{ \frac{v}{g} \left[\partial_x \varphi(x)\right]^2 + vg \left[\pi \Pi(x)\right]^2 + B_u \sin[2\varphi(x)] + B_\epsilon(x) \cos[2\varphi(x)] \Big\} . \tag{7}$$

The velocity v of the bosonic excitations is given by $v = [\pi t \sin(2\eta)]/(\pi - 2\eta)$, and $g = \pi/4\eta$, where η parameterizes the interaction according to $V = -2t\cos(2\eta)$. The terms containing B_u and B_ϵ are proportional to the dimerization and the disorder, respectively.

Generally speaking, the Hubbard model is thought to be the prototypical model to describe the interplay between kinetic energy ($\rightarrow$ delocalization) and local interaction ($\rightarrow$ localization) for electronic systems. In particular, the Hubbard chain is exactly solvable by means of the Bethe ansatz, which in fact is very useful to determine some parameters [21,22] of the Luttinger description, especially the parameters g_c and g_s. However, no closed expression can be given for these quantities in the Hubbard model (but see also next paragraph). An interaction with longer range, the more generic case, leads to even more phases in the ground state phase diagram [23]. The Hamiltonian of the Hubbard model is given by

$$H_{\mathrm{Hubb}} = -t \sum_{i,\sigma}^{N} \left(c^+_{i,\sigma} c_{i+1,\sigma} + \mathrm{h.\ c.} \right) + U \sum_{i}^{N} n_{i,\uparrow} n_{i,\downarrow} + \sum_{i,\sigma} \epsilon_i n_{i,\sigma} . \tag{8}$$

In the clean case, it shows three phases. Phase one occurs for $U < 0$, where the spin excitation spectrum has a gap – thus $g_s = 0$ – and the low-lying charge excitations can be described by those of a Luttinger liquid with $1 < g_c < 2$. Phase two arises for $U \geq 0$ and away from half filling, where spin and charge excitations are those of a Luttinger liquid with $g_s = 1$ and $1/2 \leq g_c \leq 1$. For small U, g_c is given by $g_c = 1 - U/(\pi v_F)$ in phase one and two. The last phase occurs for $U > 0$ and half filling, where the charge excitations have a gap – $g_c = 0$ – and the spin excitations are of Luttinger type with $g_s = 1$. The crucial point here is that the non-interacting electron system is unstable with respect to an attractive interaction. Moreover, non-interacting electrons are a singular point in the phase diagram for half filling. In the bosonized form, (8) can be rewritten as follows:

$$H_{\mathrm{B}} = \frac{1}{4\pi} \sum_{\mu=\mathrm{c,s}} \int \mathrm{d}x \Big\{ v_\mu \frac{\left[\partial_x \varphi_\mu(x)\right]^2}{g_\mu} + v_\mu g_\mu \left[2\pi \Pi_\mu\right]^2 + B_s \cos[2\varphi_s(x)] + B_c \cos[(4k_F - G)x + 2\varphi_c(x)] + B_\epsilon(x) \cos[\varphi_s(x)] \cos[\varphi_c(x)] \Big\} , \tag{9}$$

where G is a reciprocal lattice vector. In the clean case, H_B shows the spin-charge separation which is characteristic for Luttinger liquids. The B_s-term with

$B_s \propto U$ arises from backscattering ($q \approx 2k_F$) of two electrons with opposite spin and is responsible for the spin gap whenever $U < 0$. The B_c-term with $B_c \propto U$ arises from Umklapp scattering ($q \approx 4k_F$) of two electrons with opposite spin and generates the charge gap for $U > 0$ and half filling. In addition, the B_s-term is marginal for a repulsive interaction, thus leading to logarithmic corrections for zero magnetization. The particle-density, $n(x)$, and the magnetization, $m(x)$, of course, describe real electrons and therefore couple spin and charge,

$$n(x) = n_0 + \frac{\partial_x \varphi_c}{\pi} + \frac{k_F}{\pi} \cos[2k_F x + \varphi_c] \cos[\varphi_s] \,, \tag{10}$$

$$m(x) = \frac{\partial_x \varphi_s}{2\pi} + \frac{k_F}{2\pi} \sin[2k_F x + \varphi_c] \sin[\varphi_s] \,, \tag{11}$$

where $n_0 = N_e/N$ is the electron density; N_e is the number of electrons. The ground state magnetization, $M = \sum_i \langle s_i^z \rangle = (N_\uparrow - N_\downarrow)/2$, vanishes when no external field is present.

3 Quantum Coherence of Spinless Fermions

Using the phase sensitivity we study in the following the ground state phase diagrams with respect to the parameters interaction and potential strength.

3.1 A Single Impurity

The behavior of an interacting Fermi system in the presence of a local potential scatterer is the most studied example of an impurity effect. In this case, the free motion of the fermions inside the ring is influenced mainly by the backscattering at the impurity ($\pm k_F \to \mp k_F$). As discussed by Kane and Fisher [24] the impurity strength scales to zero (i.e. the defect becomes transparent) for an attractive interaction, and scales to infinity (i.e. it becomes completely reflective) for a repulsive interaction, according to the renormalization group equations

$$\frac{\mathrm{d}\epsilon_0}{\mathrm{d}\ln L} = (1-g)\epsilon_0 \,, \qquad \frac{\mathrm{d}}{\mathrm{d}\ln L}\frac{4t^2}{\epsilon_0} = (1-1/g)\frac{4t^2}{\epsilon_0} \,, \tag{12}$$

where L is the length of the chain. Here we consider, for example, an impurity at the end of the chain, $x = 0$. For strong ϵ_0 the transition rate – the effective hopping matrix element between the two sites next to the barrier – is given by $4t^2/\epsilon_0$. Accordingly, the phase sensitivity is given by

$$N\Delta E = \frac{\pi v g}{2} - \epsilon_0 \left(\frac{N}{N_0}\right)^{1-g} \tag{13}$$

in the case of a weak potential, and by

$$N\Delta E = \frac{4t^2}{|\epsilon_0|} \left(\frac{N}{N_0}\right)^{1-1/g} \tag{14}$$

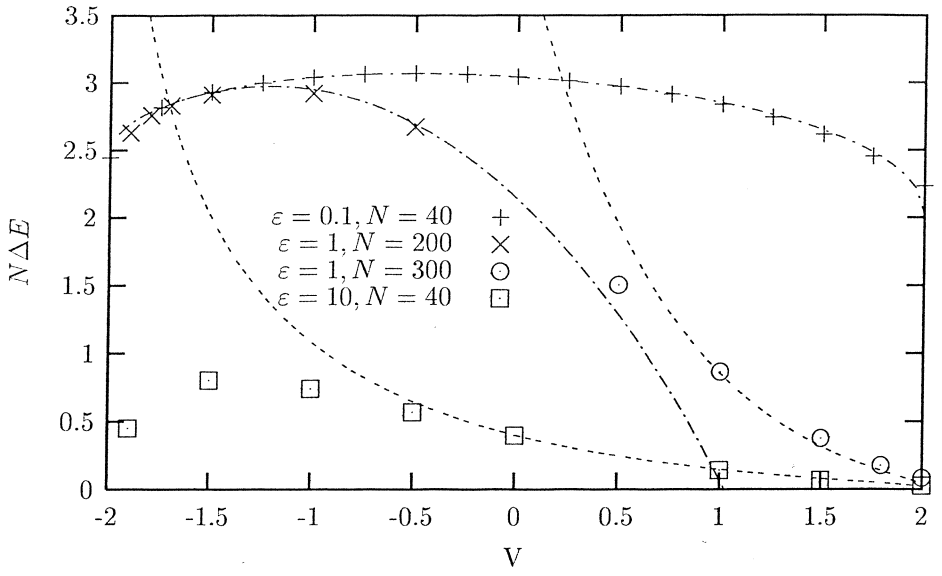

Fig. 1. Phase sensitivity as a function of interaction for a system with one impurity [7]. The lines indicate the behavior appropriate for a weak (*dash-dotted lines*) and a strong scatterer (*dashed lines*), respectively, see (13) and (14)

in the case of a strong barrier, where N_0 is a cut-off ($N_0 \approx 2$). A detailed analytical and numerical study of the phase sensitivity in the presence of a single defect can be found in [7] and [12]. For illustration we show the results for a scatterer of intermediate strength in Fig. 1, where the crossover from the weak potential to the weak link is seen for long systems. Considering a random potential or a global $2k_F$ lattice distortion instead of a local defect, the effective scaling of the perturbations qualitatively is given as follows:

$$\begin{array}{lllll} \text{local} & \langle \epsilon_0 \cos[2\varphi(0)] \rangle & \propto \epsilon_0 N^{1-g} & \to V_c = 0 \\ \text{random} & \langle \int \mathrm{d}x\, \epsilon(x) \cos[2\varphi(x)] \rangle & \propto W N^{3/2-g} & \to V_c = -1 \\ & \{\text{using } [\int \mathrm{d}x\, \epsilon(x)]^2 \sim W^2 N\} & & \\ \text{global} & \langle \int \mathrm{d}x\, u \sin[2\varphi(x)] \rangle & \propto u N^{2-g} & \to V_c = -\sqrt{2} \end{array} \tag{15}$$

The last two cases are considered below; see also [12] and [13], respectively, for details.

3.2 Random Potential

Our main results for a random potential are a universal behavior of the rms-value of the logarithmic phase sensitivity and the zero-temperature phase diagram: We find that the rms-value of the logarithmic phase sensitivity increases with system size $\propto N^{2/3}$ in the localized region; and we determine the delocalized phase which appears for an attractive interaction [12].

In the first step, generalizing the single impurity result to the case of a weak random potential, we obtain

$$\langle N\Delta E\rangle = \frac{\pi v g}{2} - \frac{W\sqrt{N_0}}{\sqrt{6\pi}}\left(\frac{N}{N_0}\right)^{(3-2g)/2}, \tag{16}$$

$$\sigma^2_{N\Delta E} = \frac{W^2 N_0}{12}\left(1-\frac{2}{\pi}\right)\left(\frac{N}{N_0}\right)^{3-2g}, \tag{17}$$

where we introduce disorder by taking the $\{\epsilon_n\}$, see (6), uniformly distributed over the interval $[-W/2, W/2]$. Again, a repulsive interaction tends to enhance the effective strength of the defects and an attractive interaction reduces it. Especially, for $g > 3/2$, i.e. $V < -1$, the strength of each defect vanishes so fast that disorder becomes an irrelevant perturbation: there is no localization. In the second step, we concentrate our discussion on the localized phase, $V > -1$. Assuming that only one relevant length scale, the localization length ξ, exists, we see that $\xi \propto W^{2/(2g-3)}$ for weak disorder. The rms-value, $\sigma_{\ln(N\Delta E)}$, for small systems is proportional to $N^{(3-2g)/2}$, see (17). A crossover is apparent in the numerical data for $N \approx \xi$, when the fluctuations of $N\Delta E$ are comparable to its average. For large systems we find the fluctuations to be proportional to $N^{2/3}$, as in the non-interacting case. Explicitly, we find from our numerical data

$$\sigma_{\ln(N\Delta E)} \approx 0.027\left(NW^{2/(3-2g)}\right)^{2/3}, \tag{18}$$

where the prefactor applies for $V = 1.2$ ($g \approx 0.71$). In summary, in the weak disorder limit, we verified quantitatively several predictions for disordered Luttinger liquids. In the localized region, we determined the localization length and the distribution of the phase sensitivity.

3.3 Periodic Potential

Including the dimerization, u, see (5), the clean spin system becomes localized by forming spin singlets on neighboring sites for $\Delta < 0$, i.e. for antiferromagnetic coupling. An excitation gap opens due to the usual Peierls mechanism [25]. Leaving aside the question whether a finite u can be stabilized, we note that the dimerization is already relevant for $\Delta < \sqrt{2}/2$ [26,27], and the ground state wave function is localized. The interaction-dimerization phase diagram was determined in [13]. The schematic phase diagram in terms of the parameters of the spinless-fermion model is shown in Fig. 2. We find – similar to the case of the random potential – for an attractive interaction a region where the distortion is irrelevant in the sense of the RG scaling. A stable dimerization, u_0, however, is only established for a repulsive interaction where the fermionic energy gain overcomes the energy loss of the lattice itself. Thereby u_0 grows with increasing interaction until the competing order of the charge density wave (CDW) – indicated by $\Delta(V)$ – sets in. Adding an impurity (dashed lines in Fig. 2) to

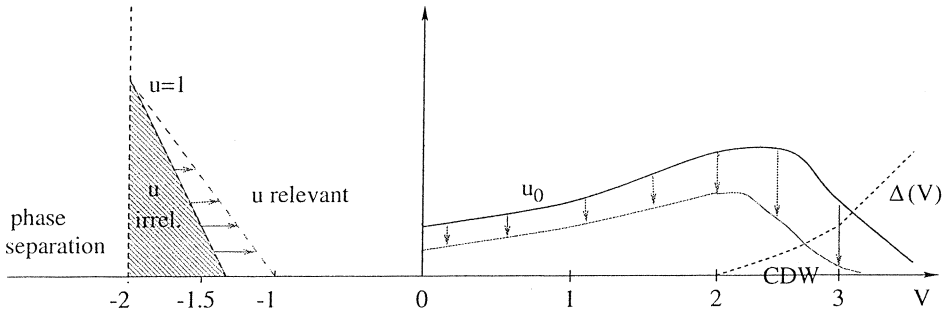

Fig. 2. Schematic ground state phase diagram of the dimerized model. The shaded region indicates a delocalized phase, where the dimerization is irrelevant. In the range $V \geq 0$ we also sketch the equilibrium dimerization u_0 and the correlation gap, $\Delta(V)$

the dimerized system the delocalized region grows [28]. On the other hand the stable dimerization and the excitation gap are reduced. In summary, the numerical results confirm the prediction of the renormalization group treatment concerning the transition point for weak distortion. In addition, it was possible to quantitatively determine the boundary of the delocalized phase for strong distortions.

3.4 Quasi-periodic Potential

Let us now consider interacting spinless fermions on a ring in the Aubry-André potential such that

$$H_{\mathrm{qp}} = -t \sum_m \left(c^+_{m+1} c_m + \mathrm{h.\ c.} \right) + V \sum_m n_{m+1} n_m + 2\mu \sum_m n_m \cos\left(\alpha m\right) . \quad (19)$$

The quasi-periodic potential shows features of both the random and the periodic potential. In the numerical analysis the value of $\alpha/2\pi$ is approximated by the ratio of successive Fibonacci numbers – $F_n = F_{n-2} + F_{n-1} = 0, 1, 2, 3, 5, 8, 13, \ldots$ – as is customary in the context of quasi-periodic systems [29]. Choosing $N = F_n$, we retain the periodicity of the quasi-periodic potential on the ring. In the non-interacting case, the one-dimensional quasi-periodic Aubry-André model is rigorously known to exhibit a metal-insulator transition for all states in the spectrum as a function of the strength of the quasi-periodic potential [9]. The ground state wave function is extended for small, and localized for large μ. At the critical value the wave functions decrease algebraically. In the case of incommensurate densities the metal-insulator transition is found at $\mu_c \approx 1$, and $N\Delta E \propto (\mu_c - \mu)^\nu$ with $\nu \approx 1$. This indicates that the influence of the interaction at this particular type of metal-insulator transition is not strong enough to change the universality class of the model. For commensurate densities, on the other hand, we find a Peierls-like behavior, similar to the situation with a periodic potential, with a metal-insulator transition at a certain value of the attractive interaction, provided μ is small. Thus, the physics of the model at commensurate densities is dominated by the Peierls resonance condition which becomes irrelevant only for a strong attractive interaction; for details see [11].

4 Local Distortions

Returning to single impurities, we discuss now Friedel oscillations in spin chains and metals. Note that the exponent of the decay of the oscillations is related to the scaling of the impurity, see (13): In case the impurity is reflecting (and thus localizing) the decay of the oscillations is expected to be slower than the x^{-1}-behavior of non-interacting particles. Otherwise, the impurity disturbs the system only locally and is thus an irrelevant perturbation.

4.1 Friedel Oscillations

Oscillations of the local density – and similarly of the magnetization – arise because the density response $n(\mathbf{q})$, given by the Lindhard function $\chi(\mathbf{q})$, is not analytic at $2k_F$. For non-interacting electrons the response function is given by [30]

$$\begin{aligned}\chi(\mathbf{q}) &= -2e^2 \int \frac{\mathrm{d}^D k}{(2\pi)^D} \frac{f(\mathbf{k}-\mathbf{q}/2) - f(\mathbf{k}+\mathbf{q}/2)}{\varepsilon(\mathbf{k}-\mathbf{q}/2) - \varepsilon(\mathbf{k}+\mathbf{q}/2)} \\ &\overset{3D}{=} -e^2 \left(\frac{mk_F}{\pi^2}\right) \left[\frac{1}{2} + \frac{1-x^2}{4x} \ln\left|\frac{1+x}{1-x}\right|\right] \qquad (20) \\ &\overset{1D}{=} -e^2 \left(\frac{2m}{\pi k_F}\right) \frac{1}{2x} \ln\left|\frac{1+x}{1-x}\right| . \qquad (21)\end{aligned}$$

Here, $x = q/2k_F$, and $f(\mathbf{k})$, $\varepsilon_{\mathbf{k}}$ denote the Fermi function and the energy of a free electron with momentum $\mathbf{k}$, respectively. The transformation to space coordinates then leads to

$$n(\mathbf{r}) \sim \cos(2\mathbf{k_F}\mathbf{r})/r^D . \qquad (22)$$

We expect that in one dimension correlation effects change the exponent of the decay,

$$n(x) = a\epsilon \frac{\cos(2k_F x)}{x^\delta} , \qquad (23)$$

where a denotes a prefactor independent of the impurity strength ϵ. In the non-interacting case it is well known that $\delta = 1 = D$. Experimentally the Friedel oscillations in a spin system can be measured by nuclear magnetic resonance spectroscopy [31]. The density oscillations of metals are more difficult to determine, but it has been reported that they can directly be observed with a scanning tunneling microscope [32]. Furthermore, oscillations in the local density of states are a signature of the Friedel oscillations too [33].

4.2 Spinless Fermions

The Friedel oscillations in a spinless-fermion system have been calculated before, analytically for repulsive interaction [34] using the bosonization technique, and

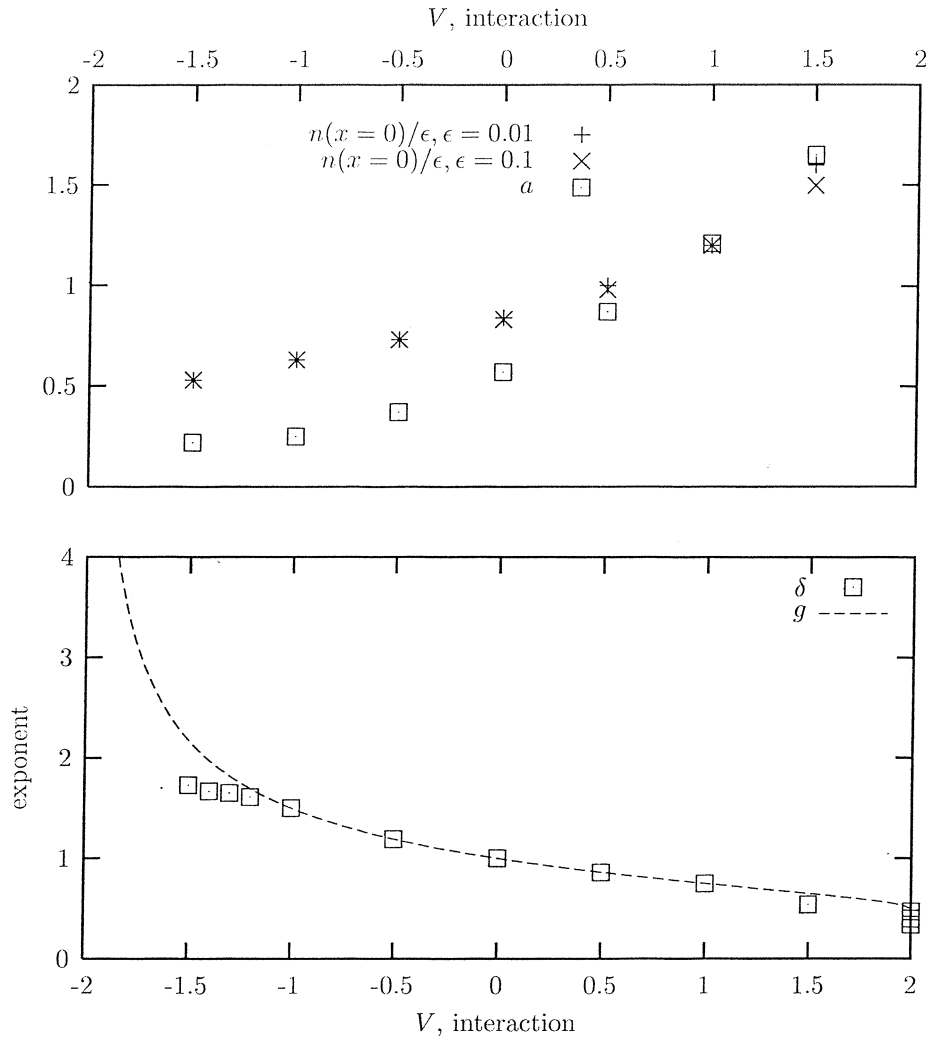

Fig. 3. The *lower panel* shows the exponent δ, obtained numerically, for half filling ($n_0 = 1/2$) versus interaction. The results are compared with the prediction $\delta = g$ from bosonization. The *upper panel* shows the local density at $x = 0$ and the prefactor a, determined for $x = 5 \ldots 20$, versus interaction

numerically for weak and intermediate interaction [35] using the DMRG. The results are confirmed by boundary conformal field theory [36]. The exponent $\delta = g$ is intimately related to the scaling relation of a single impurity, (12), mentioned above. In the case of a repulsive interaction ($g < 1$), where the impurity is relevant, the decay, x^{-g}, is slow in comparison to the increase of the system with N. In the other case ($g > 1$) where the impurity is irrelevant, the oscillations decay fast and the impurity remains local. We have determined the exponent of the decay and the prefactor of the Friedel oscillations in the Luttinger-liquid phase for a boundary defect with $\epsilon_1 = -\epsilon_N$, see [37]. In Fig. 3 (lower panel) we compare the exponent obtained numerically with the predictions from bosonization and conformal field theory. For small couplings, $-1 < V < 1$, the results are in good agreement. The deviations near $V = -2$ are related to the divergence of the Luttinger parameter g. As the impurity becomes more and more irrelevant, the oscillations die out and we find an exponential decay only.

On the other hand, at $V = 2$ the Umklapp scattering becomes marginal; therefore a logarithmic correction has to be taken into account which alters the exponent in the weak impurity case. Thus, this deviation near $V = 2$ is absent for other fillings and in the strong impurity limit. In addition, the $4k_F$-oscillations become stronger near $V = 2$. The scaling of the impurity strength according to the renormalization group equation of [24] is mainly absorbed in the exponent of the decay, i.e. the decay is slow for $V > 0$ ($g < 1$), and fast for $V < 0$ ($g > 1$). For weak impurities, a is independent of the strength of the defect while $n(x = 0)$ depends linearly on it, compare Fig. 3 (upper panel). Nevertheless, both quantities depend on interaction. They grow (due to a larger influence of the impurity) with increasing interaction. The strong impurity results, where $n(x = 0)$ saturates, are not included in Fig. 3.

4.3 Hubbard Model

We also investigate the Friedel oscillations in the one-dimensional Hubbard chain induced by boundaries and by defects, for the cases of half-filled and third-filled bands. Due to the rich phase diagram with spin-gap and charge-gap phases we compare and discuss three representative cases. Using bosonization the Friedel oscillations are given by [34]

$$\langle n(x)\rangle - n_0 \propto \frac{\cos\left(2k_F x + \psi_c\right)}{x^{(g_s+g_c)/2}}\,, \tag{24}$$

$$\langle m(x)\rangle \quad \propto \frac{\sin\left(2k_F x + \psi_s\right)}{x^{(g_s+g_c)/2}}\,, \tag{25}$$

where ψ_c and ψ_s denote arbitrary phase shifts. In the Luttinger-liquid phase a marginal operator from backscattering is always present and leads, for vanishing magnetization $M = 0$, to logarithmic corrections [38]. The Friedel oscillations in the Hubbard chain with $M \neq 0$ are considered in detail in [39].

In the first step, we analyze the numerical data assuming an algebraic decay and performing a linear regression of the log-log representation as before. We find that the exponent obtained for a defect in the middle of a chain, δ_{m}, is clearly different from the exponent obtained for a boundary defect, δ_{b}, see Fig. 4. Furthermore, both deviate from the value predicted by bosonization (≈ 0.95, see [22]). Taking into account the analysis of the marginal operator in [38], where the two relevant exponents of the logarithmic corrections were determined, we fit our data again including these corrections. Thus we determine in the second step the corrected exponents (≈ 0.95 and ≈ 0.9, see Fig. 4), which agree reasonably well with the prediction of bosonization. Of course, the logarithmic corrections of the asymptotic regime cannot be determined from our numerical results but the related deviations of the exponents on a short length scale. Increasing the impurity strength the data do not converge to the prediction from bosonization as they do in the spinless case. However, applying the logarithmic corrections we find that the oscillations decay always slower than x^{-1} in the Luttinger region, in agreement with the prediction.

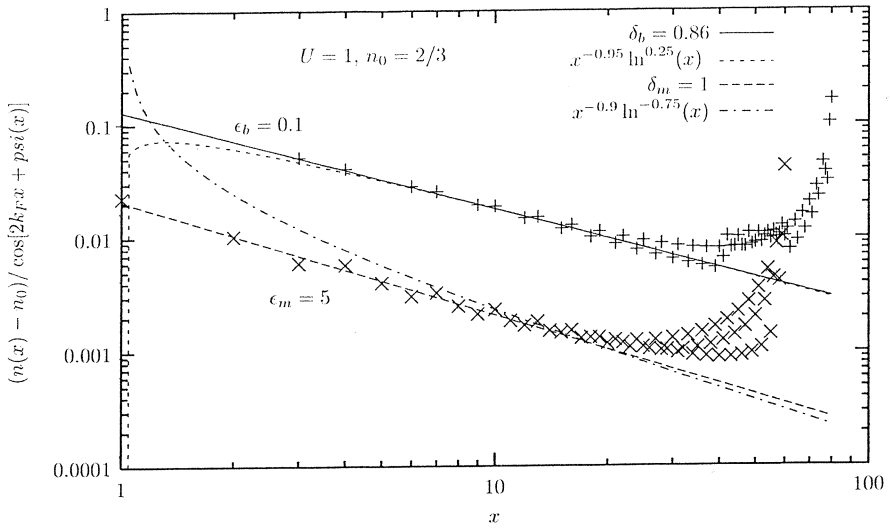

Fig. 4. Comparison of the Friedel oscillations in the Hubbard model. We set $U = 1$, $n_0 = 2/3$; the number of lattice sites is $N = 81$. The *upper curve* shows density oscillations induced by a boundary potential with $\epsilon_b = 0.1$, the *lower curve* shows the oscillations around a defect in the middle of the chain with $\epsilon_m = 5$. The data were evaluated with $\psi_c^b(x) = \pi/2$ for the boundary impurity, and with $\psi_c^m(x) = 0$ for the defect in the middle

In the phases with gap we can distinguish two cases. First we consider density (magnetization) oscillation in the spin-gap (charge-gap) phase. As seen in (10) and (11) the spin (charge) degrees couple *only* in the cosine term to the density (magnetization). Therefore we can set $g_s = 0$ ($g_c = 0$) when evaluating $\langle n(x)\rangle$ ($\langle m(x)\rangle$) and hence obtain a rather slow decay. Especially, we find $\langle m(x)\rangle \sim \cos(\pi x)x^{-0.5}$ for a strong repulsive interaction and at half filling, i.e. in the limit of the isotropic Heisenberg model. In the second case, as already stated by Luther and Emery [40] in the seventies, the decay of the density oscillations is exponential in the charge-gap phase; similarly the magnetization decreases exponentially in the spin-gap phase.

5 Summary

This article summarizes our recent theoretical studies of one-dimensional lattice models (spinless fermions, Hubbard model), which aim at a better understanding of the interplay of interaction and distortions on ground state and low-temperature transport properties. Most of our results are based on the density matrix renormalization group (DMRG) algorithm, supplemented by analytical considerations (bosonization, conformal field theory). Using the DMRG, we considered the ground state energy and the phase sensitivity of interacting spinless fermions on a ring. We found, for an attractive interaction in the presence of either a random, periodic, or quasi-periodic potential, a delocalized phase of finite extension. The zero-temperature phase diagrams have been determined.

In addition, we investigated in detail the Friedel oscillations induced by single defects. We confirmed the predictions of conformal field theory for weak interac-

tion, but near phase transitions deviations are found in the form of vanishing or additional oscillations. For the Hubbard chain, we studied these oscillations – in the density and the magnetization – in the spin-gap, charge-gap, and Luttinger-liquid phase. We found an exponential or a very slow algebraic decay of the oscillations in the gapped phases. In the Luttinger-liquid phase, we concentrated on the question of logarithmic corrections. Differences in the behavior near a boundary compared to an impurity in the bulk have been pointed out.

Acknowledgement

We thank P. Schwab for helpful discussions, and P. Brune and P. Schmitteckert for providing us with their DMRG algorithms. Financial support by the Deutsche Forschungsgemeinschaft (SPP 1073, SFB 484) is gratefully acknowledged.

References

1. B. Kramer and A. MacKinnon, Rep. Prog. Phys. **56**, 1469 (1993)
2. E. Abrahams, P.W. Anderson, D.C. Licciardello, and T.V. Ramakrishnan, Phys. Rev. Lett. **42**, 673 (1979)
3. D. Belitz and T.R. Kirkpatrick, Rev. Mod. Phys. **66**, 261 (1994)
4. S.V. Kravchenko, D. Simonian, M.P. Sarachik, W. Mason, and J.E. Furneaux, Phys. Rev. Lett. **77**, 4938 (1996); D. Simonian, S.V. Kravchenko, M.P. Sarachik, and V.M. Pudalov, Phys. Rev. B **57**, R9420 (1998)
5. C.A. Doty and D.S. Fisher, Phys. Rev. B **45**, 2167 (1992)
6. S. Eggert and I. Affleck, Phys. Rev. B **46**, 10866 (1992)
7. C. Schuster and U. Eckern, Ann. Phys. (Leipzig) **11**, 901 (2002)
8. B.S. Shastry and B. Sutherland, Phys. Rev. Lett. **65**, 243 (1990)
9. S. Aubry and G. André, Ann. Israel Phys. Soc. **3**, 133 (1980)
10. A. Eilmes, U. Grimm, R.A. Römer, and M. Schreiber, Eur. Phys. J. B **8**, 547 (1999)
11. C. Schuster, R.A. Römer, and M. Schreiber, Phys. Rev. B **65**, 115114 (2002)
12. P. Schmitteckert, T. Schulze, C. Schuster, P. Schwab, and U. Eckern, Phys. Rev. Lett. **80**, 560 (1998)
13. C. Schuster and U. Eckern, Eur. Phys. J. B **5**, 395 (1998)
14. C. Schuster, P. Brune, and U. Eckern: 'Impurities in a Hubbard-chain'. In: *High Performance Computing in Science and Engineering '01*, edited by E. Krause and W. Jäger (Springer-Verlag, Heidelberg, 2002), pp. 157–166
15. S.R.White, Phys. Rev. Lett. **69**, 2863 (1992); I. Peschel, X. Wang, M. Kaulke, and K. Hallberg, *Density-Matrix Renormalization: A New Numerical Method in Physics* (Lecture Notes in Physics, vol. 528, Springer-Verlag, Heidelberg, 1999)
16. F.D.M. Haldane, Phys. Rev. Lett. **47**, 1840 (1981)
17. J.M. Luttinger, J. Math. Phys. **4**, 1154 (1963); D.C. Mattis and E.H. Lieb, J. Math. Phys. **6**, 304 (1965)
18. A. Luther and I. Peschel, Phys. Rev. B **9**, 2911 (1974)
19. H.J. Schulz, Lecture notes from the Jerusalem Winter School on Theoretical Physics: *Correlated Electron Systems*, Dec. 1991–Jan. 1992, arXiv:cond-mat/9302006
20. V.E. Korepin, N.M. Bogoliubov, and A.G. Izergin, *Quantum inverse scattering method and correlation functions* (Cambridge University Press, Cambridge, 1993)
21. E.H. Lieb and F.Y. Wu, Phys. Rev. Lett. **20**, 2435 (1968)

22. H.J. Schulz, Phys. Rev. Lett. **64**, 2831 (1990)
23. J. Voit, Phys. Rev. B **45**, 4027 (1992)
24. C.L. Kane and M.P.A. Fisher, Phys. Rev. Lett. **68**, 1220 (1992)
25. R.E. Peierls, *Quantum Theory of Solids* (Oxford University Press, Oxford, 1955)
26. M. Kohmoto, M. den Nijs, and L.P. Kadanoff, Phys. Rev. B **24**, 5229 (1981)
27. F.C. Alcaraz and A.L. Malvezzi, J. Phys. A: Math. Gen. **28**, 1521 (1995)
28. C. Schuster and U. Eckern, Ann. Phys. (Leipzig) **8**, 585 (1999)
29. U. Grimm, Habilitationsschrift, Technische Universität Chemnitz (1999)
30. N.W. Ashcroft and N.D. Mermin, *Solid state physics*, chap. 17 (W.B. Saunders Company, Philadelphia, 1976)
31. J. Bobroff et al., Phys. Rev. Lett. **86**, 4116 (2001)
32. A. Depuydt et al., Phys. Rev. B **60**, 2619 (1999)
33. S. Eggert, Phys. Rev. Lett. **84**, 4413 (2000)
34. R. Egger and H. Grabert, Phys. Rev. Lett. **75**, 3505 (1995)
35. P. Schmitteckert, P. Schwab, and U. Eckern, Europhys. Lett. **30**, 543 (1995)
36. Y. Wang, J. Voit, and Fu-Cho Pu, Phys. Rev. B **54**, 8491 (1996)
37. C. Schuster, *Local distortions in spin chains*, to be published
38. T. Giamarchi and H.J. Schulz, Phys. Rev. B **39**, 4620 (1989)
39. G. Bedürftig, B. Brendel, H. Frahm, and R.M. Noack, Phys. Rev. B **58**, 10225 (1998)
40. A. Luther and V.J. Emery, Phys. Rev. Lett. **33**, 589 (1974)